14. P. Goldreich and W. H. Julian, *Astrophys. J.* **157**, 869 (1969).
15. R. M. Wald, *Phys. Rev. D.* **10**, 1680 (1974).
16. See Eq. 3.108 in (*13*).
17. S. L. Shapiro and S. A. Teukolsky, *Black Holes, White Dwarfs, and Neutron Stars* (Wiley, New York, 1983).
18. R. L. Znajek, *Mon. Not. R. Astron. Soc.* **179**, 457 (1977).
19. R. D. Blandford and R. L. Znajek, *ibid.*, p. 433.
20. J. Arons and J. J. Barnard *Astrophys. J.* **302**, 120 (1986); *ibid.*, p. 138.
21. T. Uchida, *Mon. Not. R. Astron. Soc.* **291**, 125 (1997).
22. C. Thompson, *ibid.* **270**, 480 (1994).
23. V. Canuto and C. Chiuderi, *Phys. Rev. D.* **1**, 2219 (1970).
24. W. H. Press and S. A. Teukolsky, *Nature* **238**, 211 (1972).
25. J. M. Bardeen, W. H. Press, S. A. Teukolsky, *Astrophys. J.* **178**, 347 (1972).
26. Ya. B. Zel'dovich, *Zh. Eks. Teor. Fiz.* **14**, 270 (1971) [transl. *JETP Lett.* **14**, 180 (1971)].
27. S. A. Teukolsky and W. H. Press, *Astrophys. J.* **193**, 443 (1974).
28. S. A. Teukolsky, *ibid.* **185**, 635 (1973).
29. $\sin\lambda = a/M$ is a convenient parameterization for Kerr black hole parameters, including $\Omega_H = \tan(\lambda/2)/2M$ and $J_H = M^2 \sin\lambda$, whose adiabatic evolution is given by $\dot{\Omega}_H = \dot{\lambda}/4M$ and $\dot{J}_H = M^2\dot{\lambda}$.
30. M. J. Rees, in *18th Texas Symposium on Relativistic Astrophysics and Cosmology*, A. V. Olinto, J. A. Frieman, D. N. Schramm, Eds. (World Scientific, Singapore, 1998), pp. 34–47.
31. T. Piran, preprint available at http://xxx.lanl.gov/abs/astro-ph/9810256.
32. T. Piran and R. Sari, in (*30*), pp. 494–496.
33. W. H. Press *Astrophys. J.* **170**, L105 (1971).
34. I gratefully acknowledge stimulating discussions with A. Toomre and J. M. Bardeen, and thank R. D. Blandford for drawing attention to reference 21. This research was supported by NASA grant NAG5-7012.

Geochemical Consequences of Increased Atmospheric Carbon Dioxide on Coral Reefs

Joan A. Kleypas,[1]* Robert W. Buddemeier,[2] David Archer,[3] Jean-Pierre Gattuso,[4] Chris Langdon,[5] Bradley N. Opdyke[6]

A coral reef represents the net accumulation of calcium carbonate ($CaCO_3$) produced by corals and other calcifying organisms. If calcification declines, then reef-building capacity also declines. Coral reef calcification depends on the saturation state of the carbonate mineral aragonite of surface waters. By the middle of the next century, an increased concentration of carbon dioxide will decrease the aragonite saturation state in the tropics by 30 percent and biogenic aragonite precipitation by 14 to 30 percent. Coral reefs are particularly threatened, because reef-building organisms secrete metastable forms of $CaCO_3$, but the biogeochemical consequences on other calcifying marine ecosystems may be equally severe.

Atmospheric CO_2 is expected to reach double preindustrial levels by the year 2065 (*1*). CO_2 research in the marine environment has focused on the ocean's role in sequestering atmospheric CO_2 (*2*, *3*), but the potential effects of the resulting ocean chemistry changes on marine biota are poorly known.

Dissolved inorganic carbon occurs in three basic forms: CO_2^* ($CO_{2(aq)}$ + H_2CO_3), HCO_3^-, and CO_3^{2-}. Under normal seawater conditions (pH 8.0 to 8.2), [HCO_3^-] is roughly 6 to 10 times [CO_3^{2-}]. When CO_2 dissolves in seawater, less than 1% remains as CO_2^*; most dissociates into HCO_3^- and CO_3^{2-}, and the acid formed by dissolution of CO_2 in seawater lowers the pH so that some CO_3^{2-} combines with H^+ to form HCO_3^-. Thus, addition of fossil fuel CO_2 decreases [CO_3^{2-}].

The seawater-mediated interaction of CO_2

[1]National Center for Atmospheric Research, Boulder, CO 80307, USA. [2]Kansas Geological Survey, University of Kansas, Lawrence, KS 66047, USA. [3]Department of Geophysical Sciences, University of Chicago, Chicago, IL 60637, USA. [4]Observatoire Océanologique, ESA 7076 CNRS-UPMC, B.P. 28, F-06234 Villefranche-sur-mer Cedex, France. [5]Lamont-Doherty Earth Observatory, Palisades, NY 10964, USA. [6]Department of Geology, Australian National University, Canberra, ACT 0200, Australia.

*To whom correspondence should be addressed. E-mail: kleypas@ncar.ucar.edu

and calcium carbonate (CO_2 + H_2O + $CaCO_3$ $\leftrightarrow$ $2HCO_3^-$ + Ca^{2+}) illustrates how addition of CO_2 enhances $CaCO_3$ dissolution and removal of CO_2 enhances its precipitation. Calcium carbonate saturation state (Ω) is

$$\Omega = \frac{[Ca^{2+}][CO_3^{2-}]}{K'_{sp}}$$

where K'_{sp} is the stoichiometric solubility product for a particular mineral phase of $CaCO_3$ [calcite (calc), aragonite (arag), or high-magnesian calcite (hmc)]. Ω is largely determined by [CO_3^{2-}] because [Ca^{2+}] is near conservative in seawater. Tropical surface waters are supersaturated ($\Omega > 1.0$) with respect to all mineral phases, but the degree of saturation varies: Ω-calc is 5 to 6, Ω-arag is 3 to 4, and Ω-hmc is 2 to 3. Under the worst case global change scenarios of the Intergovermental Panel on Climate Change (IPCC), the surface ocean will remain almost entirely supersaturated with respect to $CaCO_3$, but the decreased saturation state could result in reduced calcification rates, a shift toward calcite secretors, or a competitive advantage for noncalcifying reef organisms (*4*).

Shifts in carbonate mineralogy over geologic time appear to coincide with inferred atmospheric CO_2 concentrations (*5*), and the latitudinal trends of Phanerozoic carbonate accretion

rates correlate well with saturation state (*6*). Current reef distribution also correlates with saturation state (*7*), and large-scale biogeochemical studies have found a positive relationship between saturation state and calcification (*8*). Fragile coral skeletons have been reported from high-latitude, low Ω-arag reefs and coral communities (*9*), and reefs in well-mixed, highly supersaturated waters such as the Red Sea tend to have abundant internal carbonate cements (*10*), whereas those in low saturation waters such as the eastern Pacific have none (*11*). Modern aragonitic ooids and "whitings" also form only where Ω-arag is high (for example, Bahama Banks, Persian Gulf).

Experimental studies of calcification versus saturation state in marine organisms or communities are rare. In a recent review (*12*), six such studies on corals and marine algae (the major reef-building taxa) were identified, and, despite methodological differences, all showed a significant positive correlation between saturation state and calcification. Recent experiments in the Biosphere 2 coral reef mesocosm show a strong dependence of community calcification on saturation state (*13*).

We used two methods to predict changes in surface saturation state. The first assumed constant alkalinity through the middle of the next century and that ocean surface response to increased P_{CO_2}atm is strictly thermodynamic (P_{CO_2}surf is near equilibrium with P_{CO_2}atm) (*14*). This is valid in the tropics except for upwelling regions (*3*). The second method employed the HAMOCC (Hamburg Ocean Carbon Cycle) global model (*15*), which simulates response of the entire carbon system to increased P_{CO_2}atm and can thus be used to project further into the future. In this model biogeochemical tracers are advected with a frozen present-day climatological flow field, neglecting the possibility of future changes in ocean circulation (*16*).

Both methods indicate a significant drop in Ω-arag as P_{CO_2}atm increases (Fig. 1, A and B). The HAMOCC model Ω-arag values are consistently lower than the thermodynamic calculations because of slightly different global change scenarios and differences between modeled and measured alkalinity. Otherwise the two methods produce similar trends (Fig. 1C). Average Ω-arag in the tropics 100 years ago

was 4.6 ± 0.2 (1 SD) and is currently 4.0 ± 0.2. It is projected to drop to 3.1 ± 0.2 by the year 2065 and to 2.8 ± 0.2 by 2100 (Fig. 1C). High-saturation areas will experience the greatest decrease in saturation state (for example, Ω-arag in the Red Sea will decrease from 6.0 to 4.0 by 2100). Based on the thermodynamic calculation and the period of modern coral reef growth (since 8000 to 10,000 years ago in many cases), coral reef development is associated with an Ω-arag value of at least 4.0.

Projected changes in Ω-arag were used to predict how reef calcification might change over the next century. Changes in calcification rate (ΔG) were calculated by using the average calcification response of tropical species (12, 13) to aragonite saturation state and the thermodynamic calculations of Ω-arag. ΔG is expressed as percent of average "preindustrial" (1880) calcification rate (Fig. 2). These calculations indicate that aragonite and

high-magnesian calcite precipitation in the tropics has already decreased an average of 6% to 11% and will be another 8% to 17% lower under doubled CO_2 conditions. Total preindustrial to 2100 calcification decrease could be as high as 17% to 35%.

The expected primary effects of reduced calcification are weaker skeletons, reduced extension rates, and increased susceptibility to erosion. These primary effects will lead to a host of secondary changes in community structure, reproduction, and overall community function. If saturation state is a limiting variable with importance comparable to temperature (7), expansion of tropical sea-surface temperatures into higher latitudes (such as predicted in global warming scenarios) would not imply expanded coral reef development.

Reef building requires that organisms deposit $CaCO_3$ in excess of physical, biological, and chemical erosion. A 10% to 20% de-

crease in $CaCO_3$ production will pose a significant deficit for many coral reefs. The reefs projected to experience the greatest ΔG are those currently in high saturation conditions, such as the Red Sea, west central Pacific, and Caribbean. However, reefs with balanced $CaCO_3$ budgets ($CaCO_3$ destruction = production) are likely to be the most affected. These might include high latitude reefs (for example, Bermuda), reefs in upwelling regions (for example, Galápagos), and many reefs experiencing anthropogenic stresses.

Many uncertainties surround the issue of coral reefs and global change. Calcification versus saturation state data are scarce, and the average response presented here is only a first approximation of how coral reefs in general will respond. More studies at the ecosystem level are needed. The shape of the calcification versus saturation curve may be crucial in predicting how reefs will fare over the next 50 to 100 years. The curve used in calculating global calcification is based on a straight-line relationship, but a response curve like that of *Stylophora pistillata* (17) indicates that calcification may remain constant over a range of values and then drop precipitously below some threshold value. The response to lowered saturation could be species-specific, so that calcification rates of some species will be affected before those of others—with potentially serious consequences
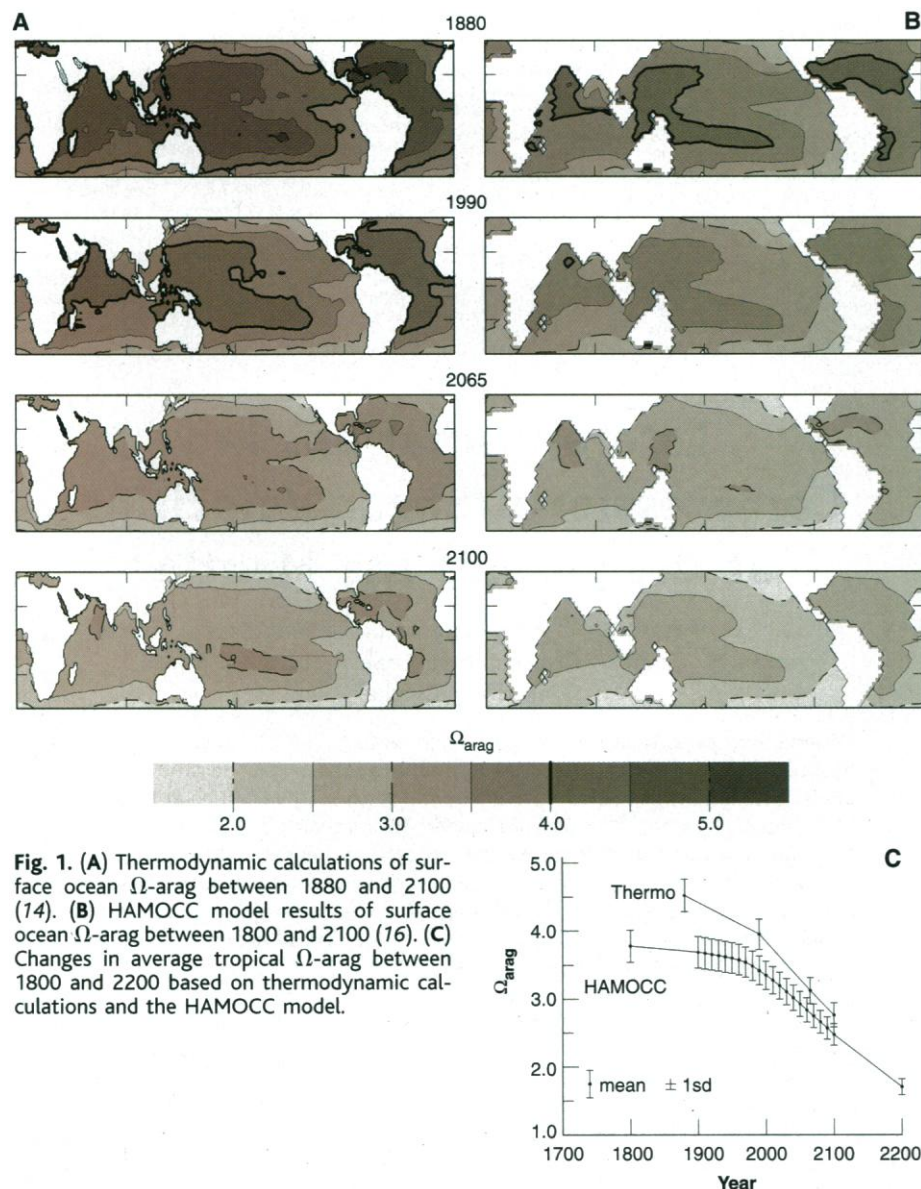

Fig. 1. (A) Thermodynamic calculations of surface ocean Ω-arag between 1880 and 2100 (14). (B) HAMOCC model results of surface ocean Ω-arag between 1800 and 2100 (16). (C) Changes in average tropical Ω-arag between 1800 and 2200 based on thermodynamic calculations and the HAMOCC model.
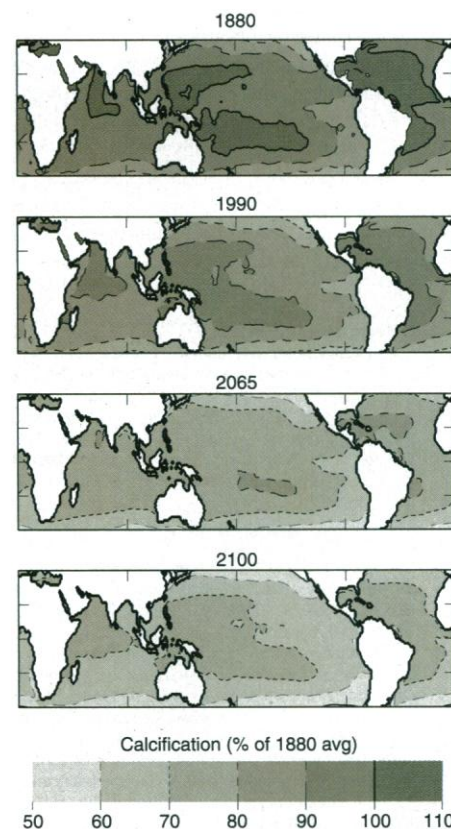
Fig. 2. Projected changes in reef calcification rate based on average calcification response of two species of tropical marine algae and one coral (12) and a marine mesocosm (13).

at community and ecosystem levels. Calcification versus saturation experiments cited here were conducted over days to weeks. Whether individual reef-building species display an acute versus chronic response to saturation state or whether they can adapt to more gradual changes in carbonate chemistry is unknown. Possible mitigative physiological effects, such as CO_2 fertilization of calcareous algae or the symbiotic algae within coral tissues, are addressed elsewhere (12). The geological record offers no evidence of either adaptation or mitigative affects; nonetheless, these considerations are important when the effects of global change on photosynthetic and calcifying organisms are being weighed.

Given the decrease in average tropical Ω-arag from 4.6 to 4.0 over the past century, net calcification has probably already decreased on some reefs. We may be able to detect such changes in coral records through either coral calcification or stable isotope records. For example, $\delta^{13}C$ and $\delta^{18}O$ in several foraminiferans correlate strongly with carbonate saturation state (18). Although reduced calcification decreases the ocean-atmospheric CO_2 flux, this effect will be small because CO_2 evasion from reef calcification is only about 1% that of present-day fossil fuel emissions (19).

The possibly dire consequences of reduced reef calcification warrant a much closer look at the biogeochemistry of shallow water carbonate secretors. Better quantification of the calcification-saturation relationship, through laboratory and field studies, and examination of geologic records are needed, as is a mechanistic understanding of calcification physiology in corals and algae (12). This analysis has focused on coral reef calcification, but other calcifying marine ecosystems (both neritic and open ocean) may share similar risks.

References and Notes

1. J. T. Houghton et al., Climate Change 1995. The Science of Climate Change (Cambridge Univ. Press, Cambridge, 1996).
2. H. Y. Inoue, M. Ishii, H. Matsueda, M. Ahoyama, I. Asanuma, Geophys. Res. Lett. 23, 1781 (1996); C. L. Sabine, D. W. R. Wallace, F. J. Millero, Eos 78, 49 (1997); N. Gruber, Global Biogeochem. Cycles 12, 165 (1998).
3. T. Takahashi et al., Proc. Natl. Acad. Sci. U.S.A. 94, 8292 (1997).
4. S. V. Smith and R. W. Buddemeier, Annu. Rev. Ecol. Syst. 23, 89 (1992); R. W. Buddemeier, Bull. Inst. Oceanogr (Monaco) 13, 119 (1994); _____ and D. G. Fautin, ibid. 14, 23 (1996); ibid., p. 33.
5. P. A. Sandberg, in The Carbon Cycle and Atmospheric CO_2: Natural Variations Archean to Present, American Geophysical Union Monograph 32, E. T. Sundquist and W. S. Broecker, Eds. (American Geophysical Union, Washington, DC, 1985), pp. 585–594; P. Sandberg, in Carbonate Cements, Society of Economic Paleontologists and Mineralogists (SEPM) Special Publication 36, N. Schneidermann and P. M. Harris, Eds. (SEPM, Tulsa, OK, 1985), pp. 33–57.
6. B. N. Opdyke and B. H. Wilkinson, Am. J. Sci. 293, 217 (1993); Palaeogeogr. Palaeoclim. Palaeoecol. 78, 135 (1990).
7. J. Kleypas, J. McManus, L. Meñez, Am. Zool. 39, 146 (1999).
8. W. S. Broecker and T. Takahashi, J. Geophys. Res. 71, 1575 (1966); S. V. Smith and R. Pesret, Pac. Sci. 28, 225 (1974).
9. C. J. Crossland, Proc. 6th Int. Coral Reef Symp. 1, 221 (1988); J. E. N. Veron, A Biogeographic Database of Hermatypic Corals (Australian Institute of Marine Science Monograph Series 10, Townsville, Australia, 1993) (although Crossland attributed lighter calcification to low temperatures or low light, or both).
10. A. K. A. Behairy and M. K. El-Sayed, Mar. Geol. 58, 443 (1984).
11. J. Cortés, Coral Reefs 16, S39 (1997).
12. Gattuso et al. [J.-P. Gattuso, D. Allemand, M. Frankignoulle, Am. Zool. 39, 160 (1999)] compiled data on two temperate coralline algae species, Bossiela orbigniana [A. D. Smith and A. A. Roth, Mar. Biol. 52, 217 (1979)] and Corallina pilulifera [K. Gao et al., ibid. 177, 129 (1973)]; two tropical coralline algae species, Amphiroa foliacea [M. A. Borowitzka, ibid. 62, 17 (1981)] and Porolithon gardineri [C. R. Agegian, thesis, University of Hawaii (1985)]; and two scleractinian corals, Stylophora pistillata and Porites compressa (F. Marubini and N. J. Atkinson, personal communication to Gattuso et al.). Our analysis excluded P. compressa (calcification response to saturation state was highest of the above species but included only two data points) and temperate species.
13. C. Langdon, T. Takahashi, T. McConnaughey, H. Anderson, H. West, paper presented at the Society for Integrative and Comparative Biology Annual Meeting, Boston, MA, January 1998. A 40% drop in calcification under double CO_2 conditions was found. Saturation state was altered by manipulating $[CO_3^{2-}]$ by adding sodium carbonate and sodium bicarbonate without changing pH.
14. Atmospheric PCO_2 and temperature were adjusted according to projections of IPCC, IS95a (1). Surface PCO_2 was adjusted by using sea-air PCO_2 differences of Takahashi et al. (3). Total alkalinity (TA) was determined as follows: TA = NTA × (salinity/35), where NTA (normalized total alkalinity) = 2306 μEq kg^{-1} [W. S. Broecker and T. H. Peng, Global Biogeochem. Cycles 3, 215 (1989)]. SST and salinity were from Levitus [S. Levitus, NOAA Professional Papers, vol. 13 (Government Printing Office, Washington, DC, 1994)], and PO_4 and SiO_2 concentrations were from Levitus et al. [S. Levitus, M. E. Conkright, J. L. Reid, R. G. Najjar, A. Mantyla, Prog. Oceanogr. 31, 245 (1993)]. $[CO_3^{2-}]$ was calculated by using standard constants for CO_2 solubility in water (K_0) [R. F. Weiss, Mar. Chem. 2, 203 (1974)] and stoichiometric constants for ionization of carbonic acid in seawater (K_1 and K_2) [F. J. Millero, Geochim. Cosmochim. Acta 59, 661 (1995)]. Phosphate and silicate were maintained at present-day levels. Ω-arag was calculated by using K'_{sp} adjusted for temperature and salinity [A. Mucci, Am. J. Sci. 283, 780 (1983)]. All calculations were done on a 1° grid.
15. E. Maier-Reimer and K. Hasselmann, Clim. Dyn. 2, 63 (1987); E. Maier-Reimer, Global Biogeochem. Cycles 7, 645 (1993).
16. Model atmosphere PCO_2 was held to 278 μatm for 1750 years while ocean chemistry adjusted to this steady state. Beginning in 1750, PCO_2atm was increased, following historical levels to the present. Future PCO_2 to the year 2200 was taken from the projection of Kheshgi et al. [H. S. Kheshgi, A. K. Jain, D. J. Wuebbles, Clim. Change 33, 31 (1996)]. Sea-surface temperature was continuously adjusted according to $\Delta T = \ln(PCO_2/ PCO_{2(init)}) \times \Delta T_{2x}$, where $\Delta T_{2x} = 2.5°C$. CO_3^{2-} concentrations were calculated as in (14), except K_1 and K_2 of Dickson and Millero [A. G. Dickson and F. Millero, Deep Sea Res. 34, 1733 (1987)] were used. The model was run on a 2.5° grid.
17. J.-P. Gattuso, M. Frankignoulle, I. Bourge, S. Romaine, R. W. Buddemeier, Global Planet. Change 18, 37 (1998).
18. H. J. Spero, J. Bijma, D. W. Lea, B. E. Bemis, Nature 390, 497 (1997).
19. J. R. Ware, S. V. Smith, M. L. Reaka-Kudla, Coral Reefs 11, 127 (1992).
20. We thank other members of the workshop Coral Reefs and Global Change: Adaptation, Acclimation, or Extinction (R. Bak, J. Benzie, B. Carlson, T. Done, R. Gates, B. Hatcher, R. Karlson, R. Kinzie III, R. Rowan, J. Pandolfi, A. Pittock, D. Potts, and S. Smith), sponsored by the Society for Integrative and Comparative Biology, Land Ocean Interactions in the Coastal Zone, Scientific Committee on Oceanic Research, and the National Oceanic and Atmospheric Administration.

Lateral Variations in Compressional/Shear Velocities at the Base of the Mantle

Michael E. Wysession,[1]* Amy Langenhorst,[2] Matthew J. Fouch,[3] Karen M. Fischer,[3] Ghassan I. Al-Eqabi,[1] Patrick J. Shore,[1] Timothy J. Clarke[4]

Observations of core-diffracted P (P_{diff}) and SH (SH_{diff}) waves recorded by the Missouri-to-Massachusetts (MOMA) seismic array show that the ratio of compressional (P) seismic velocities to horizontal shear (SH) velocities at the base of the mantle changes abruptly from beneath the mid-Pacific ($V_P/V_S = 1.88$, also the value predicted by reference Earth models) to beneath Alaska ($V_P/V_S = 1.83$). This change signifies a sudden lateral variation in material properties that may have a mineralogical or textural origin. A textural change could be a result of shear stresses induced during the arrival at the core of ancient lithosphere from the northern Pacific paleotrench.

The core-mantle boundary (CMB) is an important component of the global system of mantle convection (1), but direct observations of mantle flow at this depth have been frustratingly difficult to obtain (2). The CMB region includes a thick thermal boundary layer (labeled D''), large lateral variations at great and small scales (3, 4) that likely involve chemical boundary layers, an apparent discontinuous increase in seismic velocity 250 ± 100 km above the core (5), an ultralow-velocity zone probably attributable to partial melting (6), boundary topography, and seismic anisotropy (7). Most studies of the CMB have used observations of